

# SINTEZA NANOPARTICULELOR COMPOZITE $\text{Fe}_3\text{O}_4$ - $\text{TiO}_2$ PENTRU FOTODEGRADAREA AMPICILINEI SI PENICILINEI G

## SYNTHESIS OF $\text{Fe}_3\text{O}_4$ - $\text{TiO}_2$ COMPOSITE NANOPARTICLES FOR AMPICILLIN AND PENICILLIN G PHOTO-DEGRADATION

AURELIA CRISTINA NECHIFOR<sup>1</sup>, ABBAS ABDUL KADHIM KLAIF RIKABI<sup>1,2</sup>,  
DANIELA DUMITRA CLEJ<sup>1</sup>, SZIDONIA-KATALIN TANCZOS<sup>1,3</sup>, CORNELIU TRIȘCĂ-RUSU<sup>4</sup>,  
CRISTINA ORBECI<sup>1\*</sup>

<sup>1</sup>Universitatea Politehnica București, Str. G. Polizu nr. 1-7, 011061, București, România

<sup>2</sup>Foundation of Technical Education, Baghdad, Iraq

<sup>3</sup>Universitatea Sapientia Miercurea Ciuc, Piata Libertatii nr. 1, 530104, Harghita, România

<sup>4</sup>Institute for Research and Development in Microtechnologies, Str. Erou Iancu Nicolae nr. 126A, 077190, București, România

*This study focuses on developing a new method to obtain  $\text{Fe}_3\text{O}_4$ - $\text{TiO}_2$  nanoparticles and on their use through photocatalysis in environmental applications. The procedure for the preparation of  $\text{Fe}_3\text{O}_4$ - $\text{TiO}_2$  nanoparticles occurs according to an in situ  $\text{TiO}_2$  synthesis and magnetite covered process. After preparation, the  $\text{Fe}_3\text{O}_4$ - $\text{TiO}_2$  nanoparticles were exhaustively characterised by XRD (SAED), EDAX, TEM/HRTEM. The catalytic performances of the  $\text{Fe}_3\text{O}_4$ - $\text{TiO}_2$  nanoparticles in environmental applications, at different concentrations, were evaluated in relation to the degradation of the ampicillin and penicillin G antibiotics, using a photocatalytic reactor with continuous recirculation. The reactor was equipped with an exterior magnetic field necessary to support the  $\text{Fe}_3\text{O}_4$ - $\text{TiO}_2$  nanoparticles in the volume of the solution. Different concentrations of  $\text{Fe}_3\text{O}_4$ - $\text{TiO}_2$  nanoparticles were used. The initial concentrations of the antibiotics were equivalent to 400  $\text{mgO}_2/\text{L}$ . Monitoring the concentration of the organic substrate took place by taking off samples from the reactor, at pre-established times, and analysing them using Chemical Oxygen Demand (COD). The values for the studied process variables were: pH of the solutions at 3 and  $\text{H}_2\text{O}_2$  concentration of 1.5 per stoichiometric ratio. The effect of  $\text{Fe}_3\text{O}_4$ - $\text{TiO}_2$  in environmental applications showed good activity in a UV light, able to degrade 97.5% ampicillin and 95.0% penicillin G in 2.0 hours of reaction time.*

*Acest studiu se concentrează pe dezvoltarea unei noi metode de obținere a nanoparticulelor  $\text{Fe}_3\text{O}_4$ - $\text{TiO}_2$  și utilizarea acestora prin fotocataliză în aplicații de mediu. Procedura de preparare a nanoparticulelor  $\text{Fe}_3\text{O}_4$ - $\text{TiO}_2$  are loc în conformitate cu sinteza  $\text{TiO}_2$  in situ și acoperire cu magnetită. După preparare, nanoparticulele  $\text{Fe}_3\text{O}_4$ - $\text{TiO}_2$  au fost caracterizate exhaustiv prin XRD (SAED), EDAX, TEM/HRTEM. Performanțele catalitice ale nanoparticulelor  $\text{Fe}_3\text{O}_4$ - $\text{TiO}_2$  la diferite concentrații au fost evaluate în aplicații de mediu privind degradarea antibioticelor tip ampicilină și penicilina G folosind un reactor fotocatalitic cu recirculare continuă. Reactorul a fost echipat cu un câmp magnetic exterior necesar pentru a susține nanoparticulele  $\text{Fe}_3\text{O}_4$ - $\text{TiO}_2$  în soluție. S-au folosit diferite concentrații ale nanoparticulelor  $\text{Fe}_3\text{O}_4$ - $\text{TiO}_2$ . Concentrațiile inițiale ale antibioticelor în soluțiile de lucru au fost echivalente cu 400  $\text{mgO}_2/\text{L}$ . Monitorizarea concentrației substratului organic a avut loc prin prelevarea unor probe din reactor, la momente prestabilite și analiza acestora utilizând Consumul Chimic de Oxigen (COD). Valorile studiate pentru variabilele de proces au fost: pH-ul soluțiilor 3 și concentrația de  $\text{H}_2\text{O}_2$  1,5 față de raportul stoichiometric. În aplicațiile de mediu,  $\text{Fe}_3\text{O}_4$ - $\text{TiO}_2$  au arătat o bună activitate catalitică în lumină UV, efectul degradării antibioticelor fiind de 97,5% la ampicilină și 95,0% la penicilina G, în 2 ore de reacție.*

**Keywords:**  $\text{Fe}_3\text{O}_4$  - $\text{TiO}_2$ , Ampicillin, Penicillin G, Photocatalytic oxidation

### 1. Introduction

The progressive accumulation of more and more organic compounds in natural waters is mostly due to the development and extension of chemical technologies for organic synthesis and processing. Advanced oxidation processes (AOPs) are widely used for the removal of recalcitrant organic constituents from wastewater. In this sense, AOP type procedures are very promising technologies for treating wastewater containing non-biodegradable or hardly biodegradable organic

compounds with high toxicity [1, 2]. The water resources management exercises ever more pressing demands on wastewater treatment technologies to reduce the industrial negative impact on natural water sources. Thus, new regulations and emission limits have been imposed and industrial activities are required to seek new methods and technologies capable of effectively removing pollutants from wastewater. Advanced oxidation processes (AOPs), i.e. photochemical and photocatalytic advanced oxidation processes including UV/ $\text{H}_2\text{O}_2$ , UV/ $\text{O}_3$ , UV/ $\text{H}_2\text{O}_2/\text{O}_3$ ,

\* Autor corespondent/Corresponding author,  
E-mail: cristina27ccc@yahoo.com

UV/H<sub>2</sub>O<sub>2</sub>/Fe<sup>2+</sup>(Fe<sup>3+</sup>), UV/TiO<sub>2</sub> and UV/H<sub>2</sub>O<sub>2</sub>/TiO<sub>2</sub> can be used for the oxidative degradation of organic contaminants. A complete mineralization of the organic pollutants is not necessary, being more worthwhile to transform them into biodegradable aliphatic carboxylic acids followed by a biological process. The efficiency of the various AOPs depends both on the rate of generating free radicals and on the extent of contact between the radicals and the organic compound. The main parameters, which determine the efficiency of the oxidation process, are: the structure of the organic compounds, the hydrogen peroxide and the catalyst concentrations, the wavelength and intensity of the UV radiations, the initial solution pH and the reaction contact time [2, 3]. Advanced technologies for the wastewater treatment are required to eliminate pollution and may also increase pollutant destruction or separation processes, such as advanced oxidation methods (catalytic and photocatalytic oxidation), chemical precipitation, adsorption on various media etc. These technologies can be applied successfully to remove pollutants that are partially removed through conventional methods, e.g. biodegradable organic compounds, suspended solids, colloidal substances, phosphorus and nitrogen compounds, heavy metals, dissolved compounds, microorganisms, thus enabling the recycling of residual water [4]. The oxidation process is also controlled by the presence of other species in the reaction medium (intermediate products) in the sense that they interact with the catalyst component in a different manner. The species of reductive character accelerate the oxidation process because they reduce Fe<sup>3+</sup> (inactive) to Fe<sup>2+</sup> (active) and thus the generation of OH<sup>-</sup> radicals intensifies [5, 6]. The acid type species lower the pH of the reaction medium and can form stable complexes with Fe<sup>3+</sup> or Fe<sup>2+</sup> ions, strongly slowing the oxidation process. Also, the pH has a significant role in determining the efficiency of the Fenton and photo-Fenton oxidation processes [2]. Limitations due to the use of homogeneous catalysts, such as a limited pH range, the production of Fe containing sludge, and deactivation could be overcome by heterogeneous catalysts. A series of pharmaceuticals such as analgesics, antibiotics, steroids etc. have been detected in the water feeding systems of several countries [7, 8]. Antibiotics can be more or less extensively metabolized by humans and animals. Depending on the quantities used and their rate of excretion, they are released in effluents and reach sewage treatment plants [7-9]. Available data on antibiotics (ampicillin, erythromycin, tetracycline and penicillin groups) indicate their capability to exert toxic effects on the living organisms (bacteria, algae etc.), even at very low concentrations. These antibiotics are practically non-biodegradable, having the potential to survive sewage treatment,

leading to a persistence of these compounds in the environment and a potential for bio-accumulation [10]. Antibiotics have the potential to affect the microbial community in the sewage systems and can affect bacteria in the environment and thus disturb natural elementary cycles [9]. If they are not eliminated during the purification process, they pass through the sewage system and may end up in the environment, mainly in the surface water. The presence of antibiotics in the environment has favored the emergence of antibiotic-resistant bacteria, increasing the likelihood of infections as well as the need to find new and more powerful antibiotics. Advanced oxidation processes can be used for antibiotics degradation from wastewater or for increasing their biodegradability in the biological wastewater treatment [11, 12]. The kinetic assessment of the oxidative degradation process applied to antibiotics of the type amoxicillin, ampicillin and streptomycin (pseudo 1<sup>st</sup> degree Lagergren kinetic model) suggests that the oxidative process occurs in two successive steps, with the formation of reaction intermediates. The ratio of the 1<sup>st</sup> degree kinetic constant values corresponding to the two oxidation stages depends on the structure of the antibiotics and indicates a marked decrease in the oxidation rate in the second stage. This decrease can be attributed to the formation of reaction intermediates such as inferior organic acids with a high stability in regard to oxidation and/or blocking active catalytic centers through the formation of compounds of the Fe<sup>2+/3+</sup> species with the reaction intermediates, compounds which are inactive in the process of generating radicals [12]. As expected, antibiotic-contaminated water is incompatible with conventional biological water treatment technologies [13]. Unlike complete amoxicillin degradation, the mineralization of the organic compounds from the solution is not complete in the Fenton oxidation process due to the formation of refractory intermediates [14]. Unless antibiotics are removed from wastewaters through specific purification processes, they can affect the microbial communities in filtering systems using active sludge and, in general, the bacteria found in water, and, as a result, they can disturb the natural elementary cycles. The photocatalytic oxidation of antibiotics in aqueous solution is based on the oxidative potential of the HO radicals (2.80 V) generated in the reaction medium through photocatalytic mechanisms, in the presence of H<sub>2</sub>O<sub>2</sub> and UV radiations. The advanced oxidation processes based on the photoactivity of semiconductor-type materials can be successfully used in wastewater treatment to destroy the persistent organic pollutants, resistant to biological degradation processes. Recently, the utilization of TiO<sub>2</sub> as a catalyst for the degradation of organic pollutants in water is becoming a relevant topic in view of a possible application in economically

advantageous and environmentally friendly processes not only performed with the aim to abate pollution but also for synthetic purposes [15]. TiO<sub>2</sub> is the most attractive semiconductor because of its higher photocatalytic activity, and can be used suspended into the reaction medium or immobilized as a film on solid materials. A very promising method for solving problems concerning the photocatalyst separation from the reaction medium is to use a photocatalytic reactor in which TiO<sub>2</sub> is immobilized on a support. The immobilization of TiO<sub>2</sub> onto various supporting materials has largely been carried out via physical or chemical route [16]. Using titanium dioxide for water splitting after UV irradiation, it has been shown that this can encompass a wide range of reactions, especially the oxidation of organic compounds [17]. The study of the photodegradation for a large series of substances such as halogenated hydrocarbons, aromatics, nitrogenated heterocycles, hydrogen sulfide, surfactants and herbicides, and toxic metal ions, among others has clearly shown that the majority of organic pollutants present in waters can be mineralized or at least partially destroyed. The photocatalytic treatment of many organic compounds has been successfully achieved. The photocatalytic activity is dependent on the surface and structural properties of the semiconductor such as crystalline structure, surface area, particle size distribution, porosity, band gap and hydroxyl density [18]. The environmental applications of photocatalysis using TiO<sub>2</sub> have attracted an enormous interest over the last three decades [2]. It is well established that slurries of TiO<sub>2</sub> illuminated with UV light can degrade to the point of mineralization almost any dissolved organic pollutant. Nevertheless, photocatalysis, particularly in aqueous media, has still not found widespread commercial implementation for environmental remediation. The main hurdle appears to be the cost, which is high enough. Heterogeneous photocatalysis has become an increasingly viable technology in environmental remediation. The photocatalytic degradation utilizing titanium dioxide as a photocatalyst has several advantages in comparison to traditional water purifications and wastewater treatment methods. A photocatalytic process usually requires basic elements: a semiconductor or photocatalyst, a light source, a system of reaction and the pollutant. Ultraviolet energy produces photons that will be absorbed by the photocatalyst, thus activating it [19]. Some studies have been performed to evaluate the effects on the absorption capacity of arsenic on magnetite Fe<sub>2</sub>O<sub>3</sub> nanoparticles [20, 21]. Through diverse synthesis methods (hydrothermal, ultrasonic hydrothermal, sol-gel, coprecipitation and others), ferrite nanomaterials derived from magnetite (FeO, Fe<sub>2</sub>O<sub>3</sub>) substituting the Fe<sup>2+</sup> ion in different concentrations (0.5, 0.8, 1, 1.2, 1.5) with

Co<sup>2+</sup>, Cu<sup>2+</sup>, Ni<sup>2+</sup>, Zn<sup>2+</sup> ions were obtained [22-24]. Other iron oxides and hydroxides have been reported for their practical ability in environmental applications. Resistance to oxidation of these compounds in atmospheric conditions is an important factor [25].

In this work, we present a feasible method to obtain Fe<sub>2</sub>O<sub>3</sub>-TiO<sub>2</sub> nanoparticles through the sol-gel method and evaluate its performance to remove organic compounds, such as the antibiotics-ampicillin and penicillin G, from wastewater. The objectives of this paper are: *i.* The preparation of Fe<sub>3</sub>O<sub>4</sub>-TiO<sub>2</sub> nanoparticles occurs according to an *in situ* TiO<sub>2</sub> synthesis and magnetite covered process; *ii.* the characterization of the immobilised TiO<sub>2</sub> thin films using XRD (SAED), EDAX, TEM/HRTEM; *iii.* the study of the capacity of Fe<sub>3</sub>O<sub>4</sub>-TiO<sub>2</sub> (in different concentrations) to remove antibiotics from wastewaters.

## 2. Experimental

The proposed nanoparticles synthesis was performed in three stages: obtaining magnetite nanoparticles, polyethylene coating and functionalization with cyanuryl chloride.

### 2.1 Materials

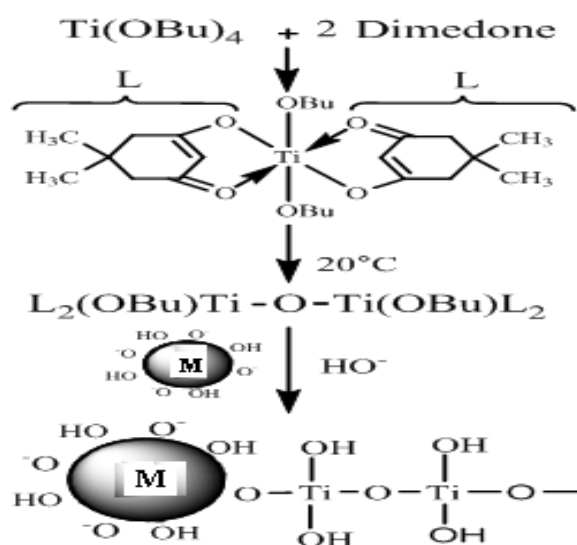
The materials used in this study are: FeC<sub>2</sub>O<sub>4</sub> (Merck), FeCl<sub>3</sub> (Fluka AG), HCl (Merck), KOH (Merck), AgNO<sub>3</sub> (Merck), *i*-butanol (Merck), titanium tetrabutoxide, Ti(OBu)<sub>4</sub> (Merck), dimedone, 5,5-Dimethyl-1,3-cyclohexanedione, C<sub>8</sub>H<sub>12</sub>O<sub>2</sub> (Merck), ampicillin and penicillin G in the form of crystalline powder of pharmaceutical grade; hydrogen peroxide, a stock solution of 30% (w/w), analytical reagent from S.C. Comchim S.A. (Bucharest, RO); sodium hydroxide analytical reagent from S.C. Chimopar S.A. (Bucharest, RO), freshly prepared with double-distilled water.

### 2.2. Procedures and Methodes

#### a. Fe<sub>3</sub>O<sub>4</sub>-TiO<sub>2</sub> composite nanoparticles synthesis

The magnetite nanoparticles were obtained through a variant of the Massart method [26-28], which consists of the coprecipitation of ferric and ferrous ions with alkali hydroxide. In a 4 L autoclave, 10 mL solution of concentration 1 mol/L FeC<sub>2</sub>O<sub>4</sub> (Merck) and 20 mL solution of 1 mol/L FeCl<sub>3</sub> (Fluka AG) were introduced, prepared in a 970 mL solution of 0.01mol/L of hydrochloric acid (Merck), precipitated with 500 mL solution of 1 M KOH (Merck), through light stirring. The dark brown precipitate was separated magnetically and inserted into a tubular membrane of regenerated cellulose (VISKING, 49 mm Φ) for continuous dialysis with bidistilled water (produced with a Millipore module) to slightly alkaline pH (7.6-8.2). After dialysis was verified the absence of chloride ions through contacting with AgNO<sub>3</sub>. The magnetite nanoparticles (M1) were coated with

titanium dioxide through the technique of in situ generation of titanium dioxide from titanium tetrabutoxide with or without the presence of dimedone [29]. Thus are activated the magnetic particles with 1 mmol KOH dispersed in 90mL of i-butanol in the 200 mL Teflon<sup>R</sup> shaft of a PM100 Retsch<sup>R</sup> colloid mill, then treated with titanium tetrabutoxide (1.11 mmol) or with a mixture of titanium tetrabutoxide (1.11 mmol) and dimedone (2.4 mmol) in 10 mL of i-butanol. After 4 hours of reaction at 250 rpm, the functionalized particles are transferred into an Erlenmeyer flask of 250 mL and are separated in a magnetic field, washed with ethanol, dried, and washed again with ethanol. Thus, types of light gray Fe<sub>3</sub>O<sub>4</sub>-TiO<sub>2</sub>, M2 composite nanoparticles are obtained, through synthesis in the absence of dimedone (Scheme I) [30].

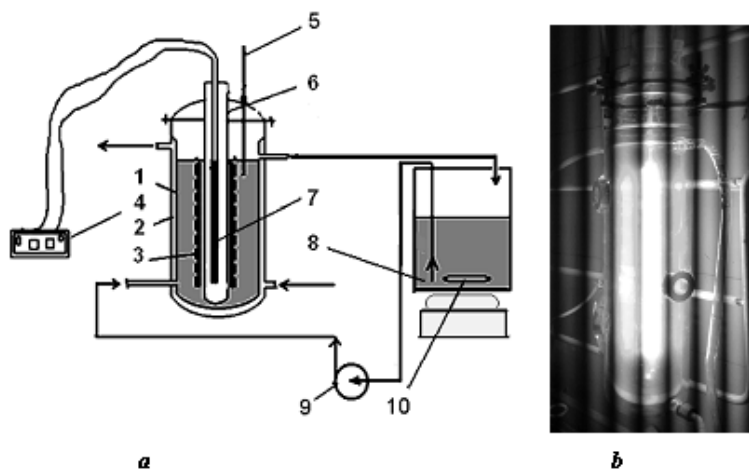


Scheme I - Reaction of coating magnetic nanoparticles with titanium dioxide in the presence of dimedone (M=magnetite) / Reacția de acoperire a nanoparticulelor magnetice cu dioxid de titan, în prezența dimedonei (M = magnetită).

The characterization of the samples obtained (M1 and M2) through electron microscopy was performed using an electron microscope through high resolution transmission (HRTEM) of the type TECNAI F30 G<sup>2</sup> STWIN with a linear resolution of 1Å and a punctual resolution of 1.4 Å [31, 32]. In the experimental research two samples of powders were analyzed, noted M1 and M2. Small amounts of powder from each sample were immersed in absolute ethanol, the suspension being homogenized through ultrasonication. For sampling, a copper grid coated with a very thin (perforated) layer of amorphous carbon was used. On this grid fine particles in homogenized suspension were collected. The samples thus taken were examined through transmission electron microscopy in bright field (TEMBF) and electron diffraction (SAED), high-resolution transmission electron microscopy (HRTEM) and energy dispersive X-ray microanalysis (EDAX), and the samples were characterized from the point of view of the nanostructure and the nanocomposition.

#### b. Evaluation of the Fe<sub>3</sub>O<sub>4</sub>-TiO<sub>2</sub> catalytic activity

The laboratory experiments for the evaluation of the Fe<sub>3</sub>O<sub>4</sub>-TiO<sub>2</sub> catalytic activity were achieved using a photocatalytic reactor [33, 34] with continuous recirculation (reaction volume 1.5 L, total solution volume 2.0 L and the recirculation flow rate 1 L/min) equipped with an electromagnetic field, a high pressure mercury lamp, of 120 W, coaxially positioned (Scheme II). The experiments were performed at 20±2°C using synthetic solutions of antibiotics (ampicillin or penicillin G) with an initial concentration equivalent to chemical oxygen demand value of 400 mg O<sub>2</sub>/L. The used amount of hydrogen peroxide ensured a 1.5 times H<sub>2</sub>O<sub>2</sub>/antibiotic stoichiometric ratio. The antibiotics oxidation processes were studied by



Scheme II: Photo-catalytic reactor representation (a) and general view in operation (b) 1-photocatalytic reactor vessel; 2-cooling jacket; 3-electromagnet, cylindrical shape; 4-UV lamp source; 5-thermometer; 6-quartz tube; 7-UV lamp; 8-recirculation reservoir; 9-recirculation pump; 10-magnetic stirrer / Reprezentarea reactorului foto-catalitic (a) vedere generală în funcțiune (b) 1- reactor foto-catalitic ;2- cămașă de răcire; 3-electromagnet, formă cilindrică; 4-sursă lampă -UV; 5-termometru;6- tubu- cuarț; 7- lampă UV; 8- rezervor recirculare; 9- pompă de recirculare; 10-agitator magnetic

monitoring the organic substrate concentration changes using chemical oxygen demand (COD) analysis function of reaction time.

The COD analyses were performed through a standard method (SR ISO 6060/1996) using a Digester DK6. In this sense, the collected samples were stabilized using  $\text{MnO}_2$  crystalline powder so that the unreacted  $\text{H}_2\text{O}_2$  could quickly decompose, and then they were filtered. For the COD analysis, the samples were corrected in terms of the pH using a NaOH solution 40% (w/w) for the Fe ions precipitation, and then they were filtered.

### 3. Results and Discussions

#### 3.1. Synthesis and characterizations of $\text{Fe}_3\text{O}_4\text{-TiO}_2$ composite nanoparticles

##### a. Magnetite nanoparticles (M1)

The structural characteristics of the magnetite sample M1, obtained using transmission

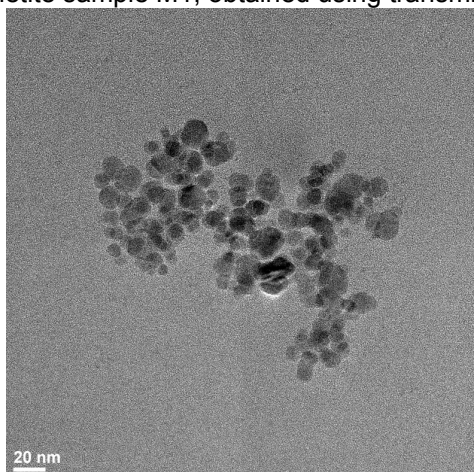


Fig. 1a- Image of transmission electron microscopy in bright field (TEMBF) presenting a set of nanoparticles / *Imagine de microscopie electronică prin transmisie în câmp luminos (TEMBF) ce prezintă un ansamblu de nanoparticule .*

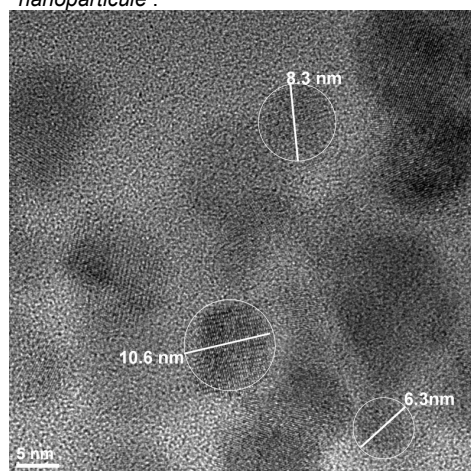


Fig. 1c- Image of high-resolution transmission electron microscopy (HRTEM) - detail from Fig. 1a / *Imagine de microscopie electronică prin transmisie de înaltă rezoluție (HRTEM) – detaliu din figura 1a.*

electron microscopy in bright field (TEMBF) are illustrated in Figure 1a [28]. As can be seen, the set consists of particles of relatively uniform sizes and shapes. It can be observed that the particles have sizes between 6 and 20 nm.

The electron diffraction pattern in Figure 1b obtained on the nano-zone in Figure 1a contains nearly diffuse diffraction spots (distributed in circles). Therefore, they correspond to very small nanocrystals. The diffraction circles correspond to the interplanar distances specified in the right of the image, distances corresponding to families of crystalline planes of Miller indices ( $hkl$ ) specified against each of the face-centered cubic lattice of the magnetite compound ( $\text{Fe}_3\text{O}_4$ ).

The image of high-resolution transmission electron microscopy (HRTEM) in Figure 1c indicates that magnetite nanoparticles are nanometer-sized, measuring between 6 nm and 11 nm, the existence of parallel fringes in each image showing that they are crystalline. The image in

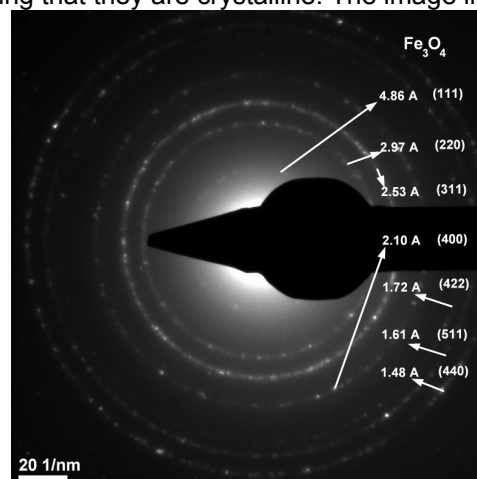


Fig. 1b- Image of electron diffraction (SAED) associated to the area in Fig. 1a / *Imagine de difracție de electroni (SAED) asociată ariei din figura 1a.*

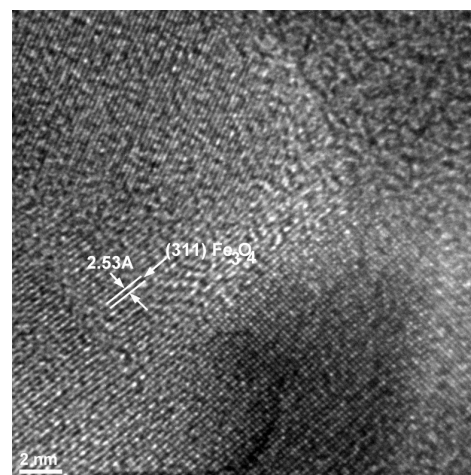


Fig. 1d- Image of high-resolution transmission electron microscopy (HRTEM) / *Imagine de microscopie electronică prin transmisie de înaltă rezoluție (HRTEM).*

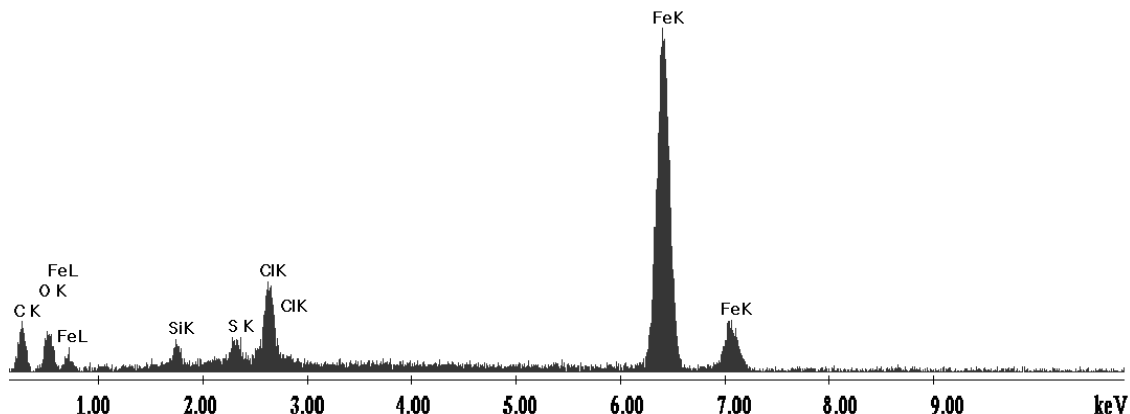


Fig. 1e. - Energy dispersive X-ray spectrum (EDAX) obtained on the nano-area from Fig. 1a / Spectrul de raze X în energie dispersată (EDAX) obținut pe nano-zona din Fig.1a.

Figure 1d highlights the existence of a crystalline ordering within these nanoparticles. In image it is measured the distance of 2.53 Å between the parallel lines corresponding to the families of crystalline planes of Miller indices (311) of the magnetite compound (Fe<sub>3</sub>O<sub>4</sub>). The energy dispersive X-ray spectrum (EDAX) in Figure 1e, shows that nanoparticles contain iron and oxygen as majority elements. The EDAX spectrum also indicates the insignificant presence of the element Si (from grinding), the element Cl (contaminant from the incomplete dialysis of these samples) and the element C (from the amorphous carbon film, from the technique of analysis).

In conclusion, the nanoparticles obtained through the selected Massart variant (M1) consist of magnetite of about 5 to 20 nm, with a crystalline structure which, after purification (for the complete removal of chloride ions) can be used in the titanium dioxide coating step.

**b. Fe<sub>3</sub>O<sub>4</sub>-TiO<sub>2</sub> (M2) composite nanoparticles (M2)**

The structural characteristics of the sample

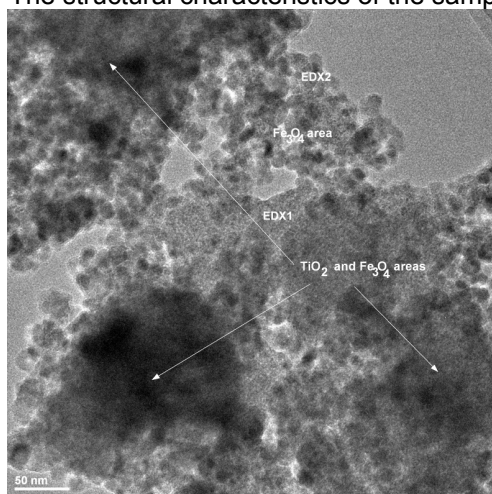


Fig. 2a- Image of transmission electron microscopy in bright field (TEM BF) presenting a set of nanoparticles / Imagine de microscopie electronică prin transmisie în câmp luminos(TEM BF) ce prezintă un ansamblu de nanoparticule.

M2, obtained through the technique of magnetite coating through the sol-gel method, without dimedone, visualized by transmission electron microscopy in bright field (TEM BF) are illustrated in Figures 2a and 2b.

Analyzing the TEM BF image (Fig. 2b), we highlight two structural aspects of the M2 sample, namely: there are regions with a structured aspect, comprising larger nanoparticles-these are areas containing a Fe<sub>3</sub>O<sub>4</sub> majority and there are regions with an indefinite, amorphous aspect, comprising much smaller nanoparticles-these are areas containing a TiO<sub>2</sub> majority. The electron diffraction pattern in Figure 2b obtained on the nano-zone in Figure 2a contains nearly diffuse diffraction spots (distributed in circles), sharper than in the case of M1. The diffraction circles correspond to the interplanar distances specified in the right of the image, distances corresponding to families of crystalline planes of Miller indices (hkl) specified against each of the face-centered cubic lattice of the magnetite compound (Fe<sub>3</sub>O<sub>4</sub>).

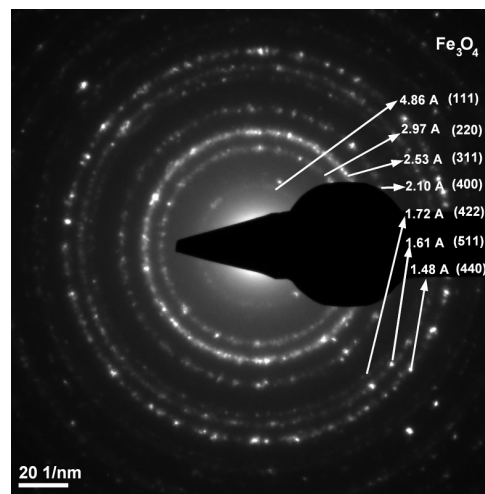


Fig. 2b- Image of electron diffraction (SAED) associated to the EDX1 area in Fig. 2a / Imagine de difracție de electroni (SAED) asociată ariei EDX1 din figura 2a.

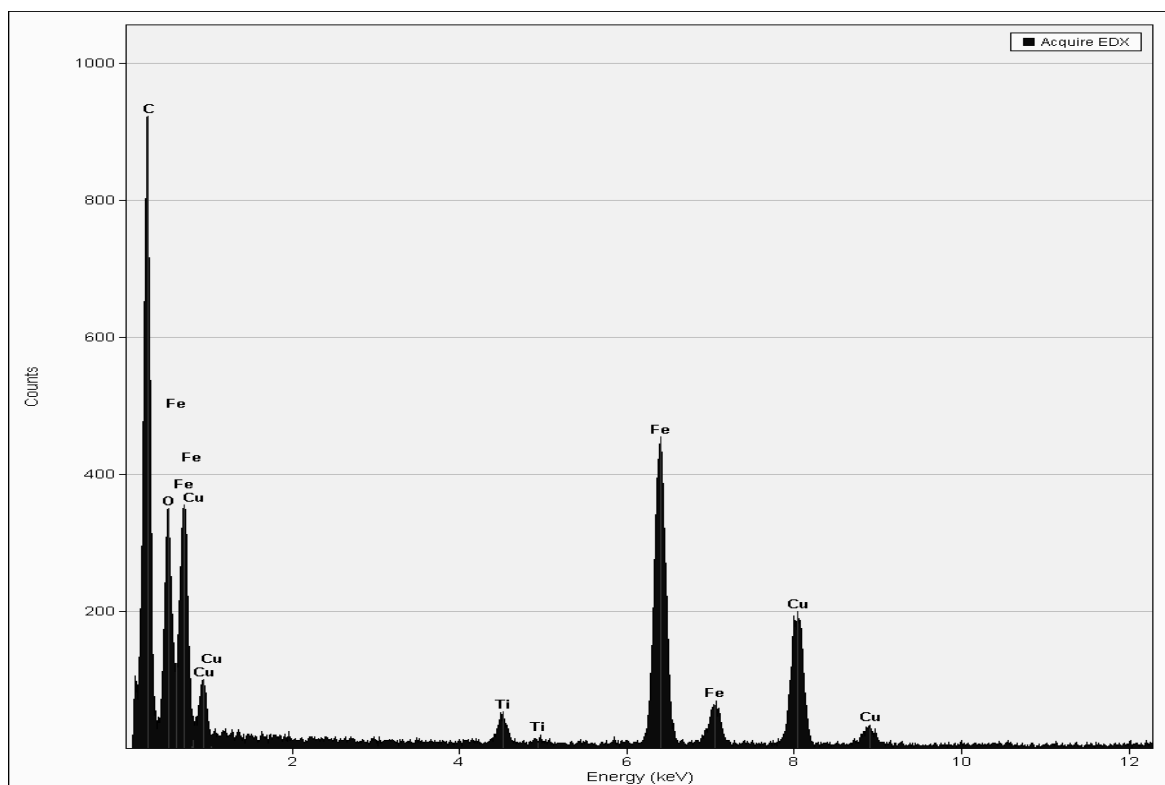


Fig. 2c- Energy dispersive X-ray spectrum (EDAX) obtained on the nano-area indicated with EDX2 in Fig.2b / Spectrul de raze X în energie dispersată (EDAX) obținut pe nanoaria indicată cu EDX2 din figura 2b.

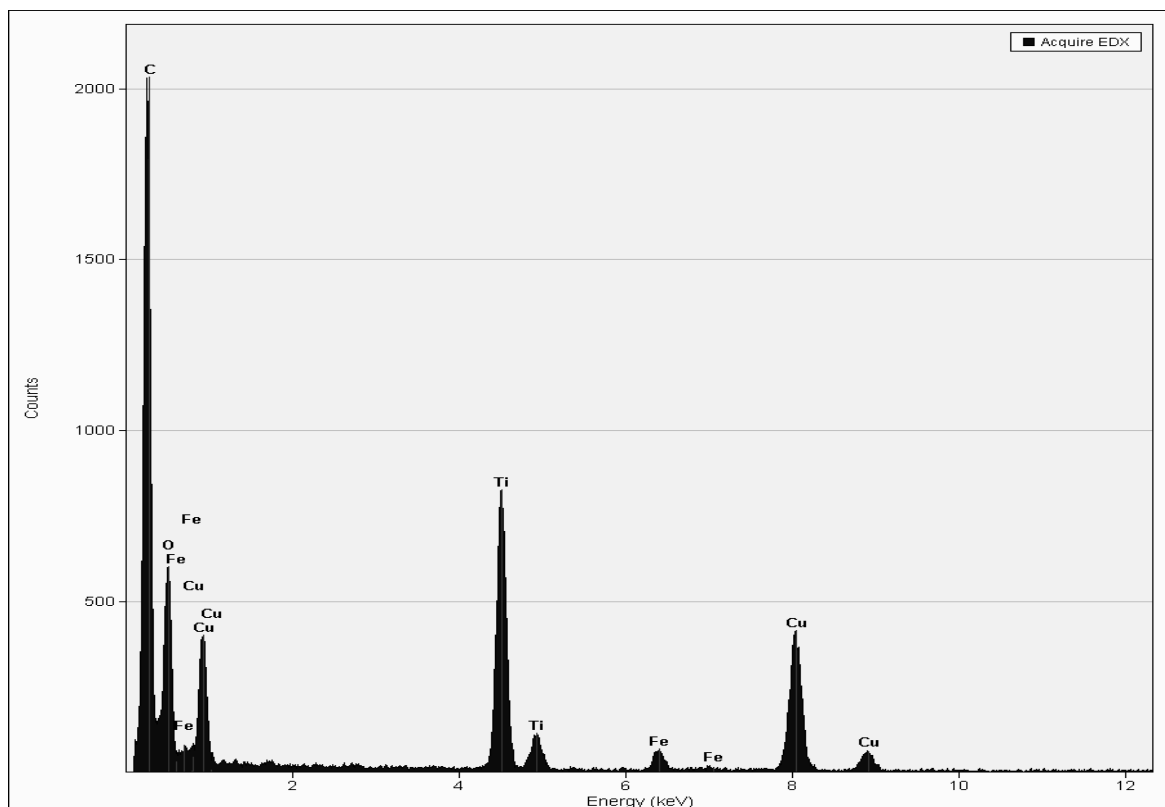


Fig. 2d- Energy dispersive X-ray spectrum (EDAX) obtained on the nano-area indicated with EDX1 in Fig.2a / Spectrul de raze X în energie dispersată (EDAX) obținut pe nanoaria indicată cu EDX1 din figura 2a.

The energy dispersive X-ray spectrum (EDAX), shown in Figure 2c, obtained on the nano-area noted in Figure 2a with EDX2, shows that the

nanoparticles in this region contain iron and oxygen as majority elements, titanium being present in a much smaller quantity. The EDAX

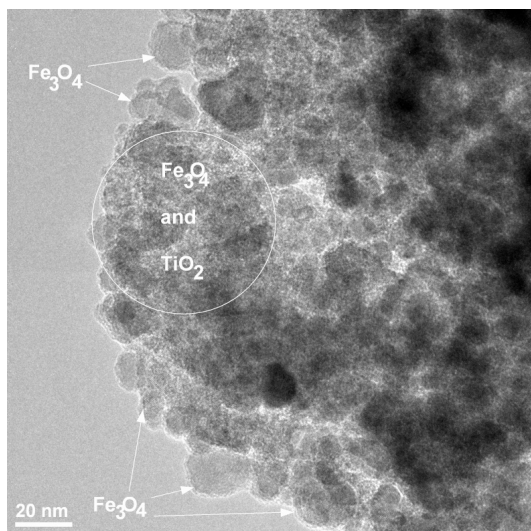


Fig. 2e -Image of transmission electron microscopy in bright field (TEM BF) presenting a set of nanoparticles; larger magnetite nanoparticles and areas with  $TiO_2$  majority / *Imagine de microscopie electronică prin transmisie în câmp luminos (TEM BF) ce prezintă un ansamblu de nanoparticule; nanoparticule mai mari de magnetită și zone cu  $TiO_2$  majoritar.*

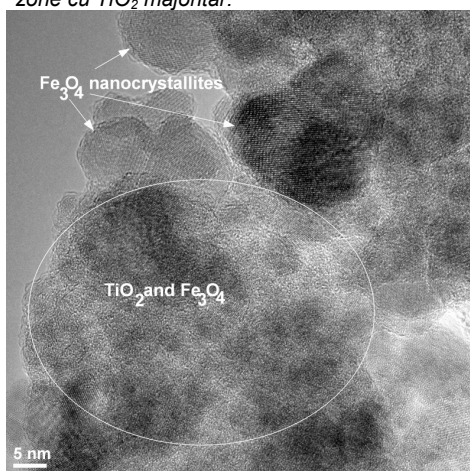


Fig. 2f- Image of high-resolution transmission electron microscopy (HRTEM) – detail from Fig. 2e / *Imagine de microscopie electronică prin transmisie de înaltă rezoluție (HRTEM) – detaliu din figura 2e.*

spectrum also shows the presence of the element Cu (the grid), and the element C (from the amorphous carbon film), as in the case of the M1 sample.

The energy dispersive X-ray spectrum (EDAX), shown in Figure 2d and obtained on the nano-area noted in Figure 2a with EDX1 indicates that the nanoparticles contain titanium and oxygen as majority elements, Fe being present in a much smaller quantity. The EDAX spectrum also shows the presence of the element Cu (the grid) and the element C (from the amorphous carbon film). The image Figure 2h highlights the existence of a crystalline ordering within the nanoparticles. In image are measured the distances of 2.53 Å and 4.86 Å between the parallel lines corresponding to families of crystalline planes of Miller indices (311) and (111) respectively, of the magnetite compound ( $Fe_3O_4$ ). In Figure 2i it is also highlighted the distance of 2.97 Å between the parallel lines corresponding to the family of crystalline planes of Miller indices (220) of the magnetite compound

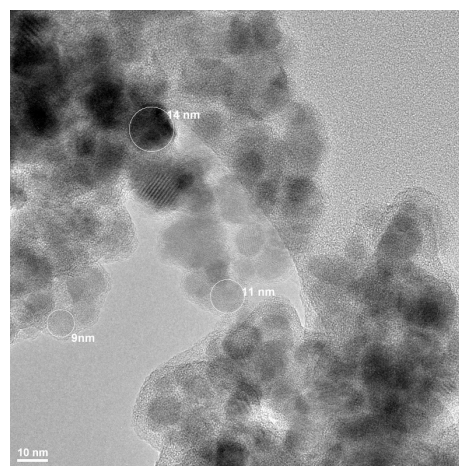


Fig. 2g- Image of high-resolution transmission electron microscopy (HRTEM) / *Imagine de microscopie electronică prin transmisie de înaltă rezoluție (HRTEM).*

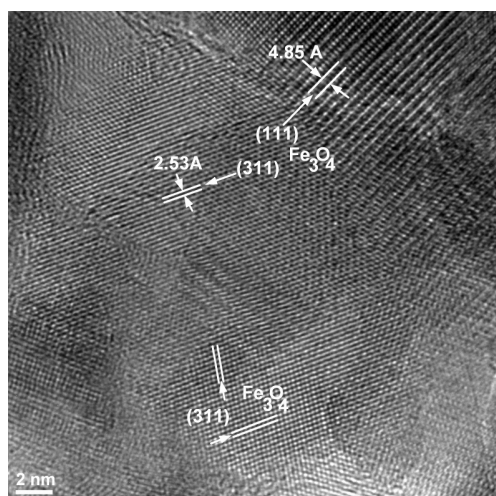


Fig. 2h- Image of high-resolution transmission electron microscopy (HRTEM) – detail from Fig. 2g / *Imagine de microscopie electronică prin transmisie de înaltă rezoluție (HRTEM) – detaliu din figura 2g.*

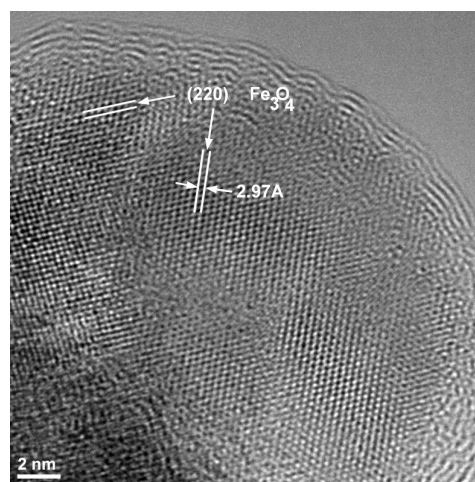


Fig. 2i- Image of high-resolution transmission electron microscopy (HRTEM) / *Imagine de microscopie electronică prin transmisie de înaltă rezoluție (HRTEM).*

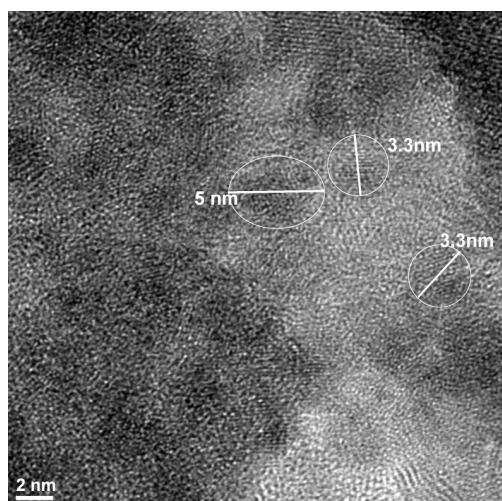


Fig. 2j- Image of high-resolution transmission electron microscopy (HRTEM); very small nanoparticles (between 3 nm and 5 nm) in the region with  $\text{TiO}_2$  majority / *Imagine de microscopie electronică prin transmisie de înaltă rezoluție (HRTEM); nanoparticule foarte mici (între 3 nm și 5 nm) în regiunea cu  $\text{TiO}_2$  majoritar*

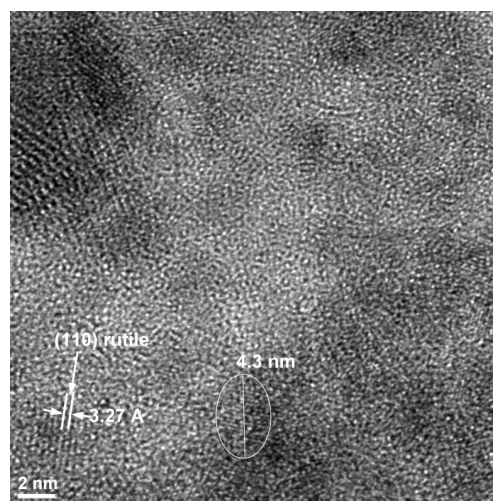


Fig. 2k- Image of high-resolution transmission electron microscopy (HRTEM); very small nanoparticle (between 3 nm and 5 nm) in the region with  $\text{TiO}_2$  majority / *Imagine de microscopie electronică prin transmisie de înaltă rezoluție (HRTEM); nanoparticule foarte mici (între 3 nm și 5 nm) în regiunea cu  $\text{TiO}_2$  majoritar*

( $\text{Fe}_3\text{O}_4$ ). It is to be noted the characteristic "core-shell" aspect. The image in Figure 2k shows the distance of 3.27 Å between the parallel lines corresponding to the family of crystalline planes of Miller indices (110) of the rutile compound ( $\text{TiO}_2$ ).

### 3.2. Environmental applications of $\text{Fe}_3\text{O}_4\text{-TiO}_2$

The photocatalytic degradation of antibiotics, such as ampicillin and penicillin G using  $\text{Fe}_3\text{O}_4\text{-TiO}_2$  was the subject of this research part. In order to attain the objective of investigating the functionalized materials prepared in environment applications, i.e. evaluating the efficiency of the  $\text{Fe}_3\text{O}_4\text{-TiO}_2$  nanoparticles in oxidative processes, we performed kinetic studies, aimed at using  $\text{Fe}_3\text{O}_4\text{-TiO}_2$  at different concentrations (0.1; 0.5; 1.0 g/L) in synthetic solutions of antibiotics and establishing the importance that the structure of the chemical compound (ampicillin or penicillin G) has on the photocatalytic process. In this sense, we used a laboratory installation for the photocatalytic oxidation of organic compounds from wastewater. The main component of this installation is the photocatalytic reactor with continuous recirculation, equipped with a UV lamp (of 120 W) and an exterior magnetic field necessary to support the  $\text{Fe}_3\text{O}_4\text{-TiO}_2$  in the whole volume of the work solution. In Figure 3a are presented the experimental data concerning the photocatalytic activity in the absence of  $\text{Fe}_3\text{O}_4\text{-TiO}_2$  compared with that in the presence of  $\text{Fe}_3\text{O}_4\text{-TiO}_2$  nanoparticles. It is to be noted that there is a clear distinction between the sets of values COD obtained in the absence of  $\text{Fe}_3\text{O}_4\text{-TiO}_2$  {tests: 1A = ampicillin + without  $\text{Fe}_3\text{O}_4\text{-TiO}_2$  + UV +  $\text{H}_2\text{O}_2$ ; 1P = penicillin G + without  $\text{Fe}_3\text{O}_4\text{-TiO}_2$  + UV +  $\text{H}_2\text{O}_2$ } and in the presence of the  $\text{Fe}_3\text{O}_4\text{-TiO}_2$  in different

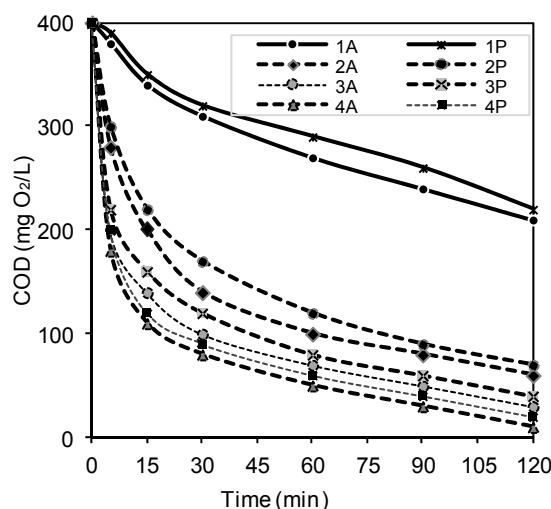


Fig. 3a - Photocatalytic activity of  $\text{Fe}_3\text{O}_4\text{-TiO}_2$  nanoparticles / *Activitatea fotocatalitică a nanoparticulelor  $\text{Fe}_3\text{O}_4\text{-TiO}_2$ .*

concentrations {tests: 2A = ampicillin + 0.1 g/L ( $\text{Fe}_3\text{O}_4\text{-TiO}_2$ ) + UV +  $\text{H}_2\text{O}_2$ ; 2P = penicillin G + 0.1 g/L ( $\text{Fe}_3\text{O}_4\text{-TiO}_2$ ) + UV +  $\text{H}_2\text{O}_2$ ; 3A = ampicillin + 0.5 g/L ( $\text{Fe}_3\text{O}_4\text{-TiO}_2$ ) + UV +  $\text{H}_2\text{O}_2$ ; 3P = penicillin G + 0.5 g/L ( $\text{Fe}_3\text{O}_4\text{-TiO}_2$ ) + UV +  $\text{H}_2\text{O}_2$ ; 4A = ampicillin + 1.0 g/L ( $\text{Fe}_3\text{O}_4\text{-TiO}_2$ ) + UV +  $\text{H}_2\text{O}_2$ ; 4P = penicillin G + 1.0 g/L ( $\text{Fe}_3\text{O}_4\text{-TiO}_2$ ) + UV +  $\text{H}_2\text{O}_2$ }.

Monitoring the concentration of the organic substrate indicated a decrease in the COD values. Also, the results obtained highlight the importance of the catalytic component ( $\text{Fe}_3\text{O}_4\text{-TiO}_2$  nanoparticles) in the system. As shown, the rates

of the organic compounds degradation increased progressively with increasing the concentration of the catalyst in the solution. The presence of the catalyst ( $Fe_3O_4-TiO_2$ ) is beneficial to the process of advanced degradation of the organic compounds in wastewaters. Essentially, the functionalized nanomaterials ( $Fe_3O_4-TiO_2$ ) show a catalytic activity, the degradation rates of the organic compounds being dependent on the reaction time. All tests related to the influence of catalyst concentration show a good photocatalytic activity in the degradation of antibiotics; the degree of oxidation increased progressively with increasing levels of nanomaterials functionalized in the working solution. The catalytic behaviour is similar (as shown by consecutive experiments); an increase is noticed in the efficiency of the photo-oxidative degradation process when the catalyst concentration in the solution increases, for prolonged UV exposure. The structure of the chemical compound (ampicillin or penicillin G) is closely related to the oxidation of organic compounds from wastewater. The efficiency to removal of organic compound, determined at the same reaction time, indicate a small variation in all tests with the  $Fe_3O_4-TiO_2$  particles (Fig. 3b).

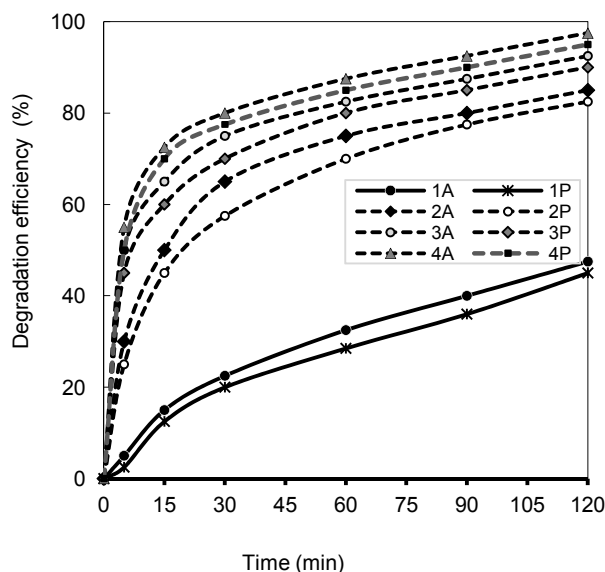


Fig. 3b - Effect of  $Fe_3O_4-TiO_2$  in environmental applications  
*Efectul  $Fe_3O_4-TiO_2$  în aplicații de mediu.*

Thus, coupling the  $Fe_3O_4$  particles with  $TiO_2$  ensures the efficiency to degradation of the organic compounds present in the solution, especially when the catalyst concentration in the solution increases. As the experimental data show in Figure 3, both the importance of structure of the chemical compound (ampicillin or penicillin G) and the catalyst concentration can be established. The presence of  $Fe_3O_4-TiO_2$  in the system is beneficial;

the antibiotics show a higher degree of degradation once with increasing the concentration of  $Fe_3O_4-TiO_2$ , from 0.1-0.5 up to 1.0 g/L. The best results were obtained when testing  $Fe_3O_4-TiO_2$  particles in a concentration equivalent to 1.0 g/L, in an ampicillin solution. It is to be noted that the photocatalytic process is stronger for ampicillin than for penicillin G, thus the oxidation rate for ampicillin is better than for penicillin G; degradations of 97.5% ampicillin and 95.0% penicillin G in 2.0 hours of reaction time were obtained.

#### 4. Conclusions

The technique proposed for obtaining  $Fe_3O_4-TiO_2$  leads to obtaining nanoparticles with magnetic and catalytic properties, stable in an oxidative medium. The advantage of this new method to obtain  $Fe_3O_4-TiO_2$  nanoparticles derives from the fact that it is a simple procedure, based on commercial raw materials with relatively low price. The main factors, which determine the characteristics of the  $Fe_3O_4-TiO_2$  nanoparticles (including mechanical strength, chemical stability, photocatalytic activity), are:  $TiO_2$  powder characteristics,  $Fe_3O_4$  characteristics, the mass ratio between  $Fe_3O_4-TiO_2$  and the thermic treatment. The  $Fe_3O_4-TiO_2$  nanoparticles showed a good photocatalytic activity and stability in the oxidation process of antibiotics. While Fe, and  $Fe_3O_4$  respectively, play an adsorption role for antibiotics,  $TiO_2$  is considered responsible for the photocatalytic activity. Therefore, the use  $Fe_3O_4-TiO_2$  in environment applications is viable.

#### Acknowledgments

The work has been funded by the Sectorial Operational Programme Human Resources Development 2007-2013 of the Ministry of European Funds through the Financial Agreement POSDRU/159/1.5/S/132395. Dr. Eugen Vasile many thanks for TEM and HRTEM interpretation support.

#### REFERENCES

1. A.G. Trovó, R.F.P. Nogueira, A. Agüera, A.R. Fernandez-Alba and S. Malato, "Degradation of the antibiotic amoxicillin by photo-Fenton process—chemical and toxicological assessment," *Wat. Res.*, 2011, **45** (3), 1394.
2. P. R. Gogate, A. B. Pandit, A review of imperative technologies for wastewater treatment I: oxidation technologies at ambient conditions, *Adv. Environ. Res.*, 2004, **8** (3), 553.
3. U.I. Gaya, A. H. Abdullah, Heterogeneous photocatalytic degradation of organic contaminants over titanium dioxide: a review of fundamentals, progress and problems, *J. Photochem. Photobiol. C: Photochem. Rev.*, 2008, **9** (1), 1.
4. H. Zhou, D.W. Smith, Advanced technologies in water and wastewater treatment, *J. Environ. Eng. Sci.*, 2002, **1** (4), 247.
5. Y. Du, M. Zhou, L. Lei, Role of the intermediates in the degradation of phenolic compounds by Fenton-like process, *J. Hazard. Mater.*, 2006, **136** (3), 859.

6. A. Riga, K. Soutsas, K. Ntampeglitis, V. Karayannis, G. Papapolymerou, "Effect of system parameters and of inorganic salts on the decolorization and degradation of Procion H-exl dyes. Comparison of H<sub>2</sub>O<sub>2</sub>/UV, Fenton, UV/Fenton, TiO<sub>2</sub>/UV and TiO<sub>2</sub>/UV/H<sub>2</sub>O<sub>2</sub> processes," *Desal.*, 2007, **211** (1-3), 72 .
7. J.P. Bound, N. Voulvoulis, Pharmaceuticals in the aquatic environment--a comparison of risk assessment strategies. *Chemosph.*, 2004, **56** (11), 1143.
8. R. Alexy, T. Kumpel, K. Kummerer, Assessment of degradation of 18 antibiotics in the Closed Bottle Test *Chemosph.*, 2004, **57** (6), 505.
9. K. Kummerer, Antibiotics in the aquatic environment – A review *Chemosph.*, 2009, **75** (4), 417.
10. I. Arslan-Alaton, A.E. Caglayan, Toxicity and biodegradability assessment of raw and ozonated procaine penicillin G formulation effluent *Ecotox. Environ. Safe.*, 2006, **63** (1), 131.
11. O. Rozas, D. Contreras, M.A. Mondaca, M., Mansilla, H.D. Pérez-Moya, Experimental design of Fenton and photo-Fenton reactions for the treatment of ampicillin solutions, *J. Hazard. Mater.*, 2010, **177** (1-3), 1025.
12. C. Orbeci, I. Untea, A.M. Dancila, D.S. Stefan, Kinetics considerations concerning the oxidative degradation by photo-Fenton process of some antibiotics, *Environ. Eng. Manag. J.*, 2010, **9** (1), 1.
13. E. Elmolla, M. Chaudhuri, Degradation of the antibiotics amoxicillin, ampicillin and cloxacillin in aqueous solution by the photo-Fenton process, *J. Hazard. Mater.*, 2009, **172** (2-3), 1476.
14. F. Ay, F. Kargi, Advanced oxidation of amoxicillin by Fenton's reagent treatment, *J. Hazard. Mater.*, 2010, **179** (1-3), 622.
15. G. Mele, I. Pio, A. Scarlino, E. Bloise, et al., New Porphyrin/Fe-Loaded TiO<sub>2</sub> Composites as Heterogeneous Photo-Fenton Catalysts for the Efficient Degradation of 4-Nitrophenol, *J. Catal.*, Article ID 376078, 7 pages, 2013, <http://dx.doi.org/10.1155/2013/376078>.
16. U.I. Gaya, A. H. Abdullah, Heterogeneous Photocatalytic Degradation of Organic Contaminants over Titanium Dioxide: A Review of Fundamentals, Progress and Problems *J. Photochem. Photobiol. C: Photochem. Rev.*, 2008, **9** (1), 1.
17. C. Lazau, P. Sfirloaga, C. Orha, C. Ratiu, I. Grozescu, "Development of a novel fast-hydrothermal method for synthesis of Ag-doped TiO<sub>2</sub> nanocrystals" *Mater. Lett.*, 2011, **65** (2), 337 .
18. S. Ahmed, M. G. Rasul, W. N. Martens, R. Brown, M. A. Hashib, Heterogeneous photocatalytic degradation of phenols in wastewater: A review on current status and developments, *Desal.*, 2010, **261** (1-2), 3.
19. A. Mansor, Photocatalytic degradation of phenol in aqueous solution using Fe/TiO<sub>2</sub> thin films under UV and visible light, Thesis submitted in fulfillment of the requirements for the degree of Master of Science, (2008).
20. S. Yean, L. Cong, Effect of magnetite particle size on adsorption and desorption of arsenite and arsenate. *J. Mater. Res.*, 2005, **20** (12), 3255.
21. X.H. Sun, H.E. Doner, An investigation of arsenate and arsenite bonding structures on goethite by FTIR" *Soil Sci.*, 1996, **161** (12), 865.
22. P.C. Fannin, C.N. Marin, I. Malaescu, et al., Effect of the concentration of precursors on the microwave absorbent properties of Zn/Fe oxide nanopowders *J. Nanopart. Res.*, 2011, **13** (1), 311.
23. P. Vlazan, M. Vasile, Synthesis and characterization CoFe<sub>2</sub>O<sub>4</sub> nanoparticles prepared by the hydrothermal method. *Optoelecton. Adv. Mat.-R. Comm.*, 2010, **4** (9), 1307.
24. N.H. Hai, N.D. Phu, Arsenic removal from water by magnetic Fe<sub>1-x</sub>Co<sub>x</sub>Fe<sub>2</sub>O<sub>4</sub> and Fe<sub>1-x</sub>Ni<sub>y</sub>Fe<sub>2</sub>O<sub>4</sub> nanoparticles, *VNU J. Sci., Math.-Phys.*, 2009, **25** (1), 15 .
25. N.H. Hai, N.D. Phu, N. Chau, H.D. Chinh, L.H. Hoang, D.L. Leslie-Pelecky, *J. Korean Phys. Soc.*, 52 (5), 1327 (2008).
26. A.C. Nechifor, M.G. Stoian, S.I. Voicu, G. Nechifor, Modified Fe<sub>3</sub>O<sub>4</sub> colloidal dispersed magnetic particles as carrier in liquid membranes, *Optoelectronics and Advanced Materials – Rapid Communications*, 2010, **4** (8), 1118.
27. V.I. Luntraru, O. Gales, L. Iarca, E. Vasile, S.I. Voicu, A.C. Nechifor, "Synthesis and characterization of dye adsorbed onto titanium dioxide magnetite composite", *Optoelectronics and Advanced Materials – Rapid Communications*, 2011, **5** (11), 1229.
28. A.C. Nechifor, L.D. Ghindeanu, C. Orbeci, O. Dorca, E. Eftimie-Totu, Magnetite-polyethyleneglycol-cyanuryl chloride reactive nanoparticles, *Romanian Journal of Materials*, 2013, **43** (3), 285.
29. V.I. Luntraru, D. I. Vaireanu, D. L. Ghindeanu, G. Nechifor, The synthesis and characterization of a new composite material: Polysulfone-Fe<sub>3</sub>O<sub>4</sub>/TiO<sub>2</sub>, *UPB Sci. Bull., B: Chem. Mater. Sci.*, 2013, **75** (2), 91.
30. V.I. Luntraru, C.M. Baicea, C. Trișcă-Rusu, A.C. Nechifor, The synthesis and characterization of new magnetic particles: iron particles covered with titanium dioxide and functionalized with cyanuric chloride, *Romanian Journal of Materials*, 2012, **42** (3), 306.
31. E. Vasile, S. Mihaiu, R. Plugaru, Scanning transmission electron microscopy investigation of ZnO:Al based thin film transistors, *Digest Journal of Nanomaterials and Biostructures* 2013, **8** (2), 721.
32. E. Vasile, F. Dumitru, A. Razvan, O. Oprea, C. Andronescu, Novel ureido-4'-aminobenzo-15-crown-5-ether periodic mesoporous silicas, *Digest Journal of Nanomaterials and Biostructures*, 2013, **8** (1), 433.
33. C. Orbeci, I. Untea, R. Stanescu, A.E. Segneanu, M.E. Craciun, A new photo-Fenton procedure applied in oxidative degradation of organic compounds from wastewater, *Environ. Eng. Manag. J.*, 2012, **11** (1), 141 .
34. C. Orbeci, I. Untea, G. Nechifor, A.E. Segneanu, M.E. Craciun, Effect of a modified photo-Fenton procedure on the oxidative degradation of antibiotics in aqueous solutions *Sep. Purif. Technol.*, 2014, **122**, 290.

\*\*\*\*\*